COMPUTER-AIDED CIVIL AND INFRASTRUCTURE ENGINEERING   WILEY

A hybrid metaheuristic method for optimization of active tuned mass dampers

Aylin Ece Kayabekir[1] | **Sinan Melih Nigdeli[2]** | **Gebrail Bekdaş[2]**

[1] Department of Civil Engineering, Istanbul Gelişim University, Istanbul, Turkey

[2] Department of Civil Engineering, Istanbul University - Cerrahpaşa, Istanbul, Turkey

Correspondence
Gebrail Bekdaş, Department of Civil Engineering, Istanbul University–Cerrahpaşa, Avcılar, Istanbul, Turkey.
Email: bekdas@istanbul.edu.tr

Abstract

A metaheuristic-based tuning methodology for the optimization of active tuned mass dampers (ATMDs) is presented. The methodology considers both physical parameters of ATMDs and controller parameters of the control algorithm. The employed control algorithm is a proportional–integral–derivative type controller. ATMDs are used in structures in the reduction of structural responses resulted from earthquakes. The proposed methodologies must be feasible for real practices in construction, so consider all physical factors such as stroke capacity, limitation of the active control force, the time delay of the generated control signal, and a time-saving one. A novel hybrid metaheuristic algorithm that combines the specific advantages of four metaheuristics (harmony search, flower pollination algorithm, teaching-learning-based optimization and Jaya algorithm) is proposed for the optimization process. The results of the process showed that ATMDs are more effective for high values strike limitations, compared to TMDs. The feasibility and effectiveness of the optimum control method are also demonstrated on a full-size 76-story structure.

1 | INTRODUCTION

Structural methods using active control systems currently have great importance as a current interest, although studies about the active control of structures with integrated optimization methods have been proposed since the 1990s. In this period, major optimization algorithms for active control of structures, including an integrated optimization method using parallel algorithms by Saleh and Adeli (1994), high-performance parallel algorithms by Saleh and Adeli (1998), and an iterative approach for finding optimum parameters of active and passive control systems based on H_2/H_∞ by J. Lu and Skelton (1998), were suggested. In the 2000s, the active control system gains more interest than before, and it is seen by the increase of approaches that were carried out. Under wind and earthquake excitations, the placement effects of control equipment on space structures were investigated by Arfiadi and Hadi (2000) for passive and active systems. Bakioğlu and Aldemir (2001) presented a method to be used in the sub-optimal solution of a closed-open-loop control that predicts earthquakes via the usage of the Kalman filter and Taylor series. An approximate optimal closed-open-loop control method was also proposed by Aldemir et al. (2001) to predict near-future excitations. Aldemir and Bakioglu (2001) applied an analytical solution for the modified linear quadratic regulator (LQR). Nomura et al. (2007) presented an active control method that combines fuzzy logic and particle swarm optimization (PSO). The technique, which is developed to improve the structural performance against earthquake vibrations, consisted of two fuzzy active control systems called fuzzy ensemble system and gating network. A dynamic fuzzy wavelet neuroemulator, which is one of the nonlinear control

models, for three-dimensional irregular structures was also used by Jiang and Adeli (2008). In the design of active control systems considering time delay, Chang and Lin (2009) suggested using a control method using the optimal H_∞ algorithm, and it is aimed to reduce the value of inter-story drift of seismic structures. An advanced version of their previous method called a multi-input, multi-output control system have been also used for vibration control of small-scale building under seismic excitations by Y. Kim et al. (2010). Numerical analyses have been performed by Lin et al. (2010) for the active control of structures with torsional irregularity considering soil-structure interaction (SSI). Nigdeli and Boduroğlu (2013) proposed a numerical iteration method for three-dimensional structures controlled by active tendon control systems using proportional–integral–derivative (PID) type controllers. Wang and Adeli (2015a) developed a robust structural control method using sliding mode control of wind-excited high-rise buildings by finding the control force according to the equivalent control force principle. Z. Li and Adeli (2016) proposed a novel discrete-time robust H_2/H_∞ control algorithm that is robust against parametric uncertainties of buildings. Gutierrez Soto and Adeli (2017a) proposed a multi-objective Pareto optimization for control systems by using the neural dynamics model of Adeli and Park (1995). Soto and Adeli (2018) optimized smart base-isolated irregular buildings by using a multi-objective optimization using the neural dynamics model to provide the Pareto optimal replicator parameters. Then, Soto and Adeli (2019) conducted the control method based on game theory and replicator dynamic for a hybrid system combining isolation systems with semi-active control devices used for bridge structures. Detailed literature survey on structural control methods can be found in Soto and Adeli (2017b) and Z. Li and Adeli (2018).

Active tuned mass damper (ATMD) studies related to the scope of this study are also summarized as follows. Ankireddi and Yang (1996) utilized a full feedback control algorithm that includes displacement, velocity, and acceleration feedback in the design of the ATMD system for tall structures under wind effects. In the investigation done by Mackriell et al. (1997), the proposed acceleration feedback control algorithm was proved effective in reducing the first-mode vibration of tall structures due to wind loads. Yan et al. (1999) introduced a norm control technique using root mean square responses (Hrms) to test analytical expressions derived by Ankireddi and Yang (1996) for the optimal feedback gain of ATMD under both along-wind and across-wind excitations. According to the test results, the method proposed by Ankireddi and Yang (1996) is suitable to obtain optimum design parameters under along-wind excitations, while the optimum frequency ratio was not found by the method for the cross-wind excitations. Qu

et al. (2001) used a dynamic method that is a kind of system reduction scheme to obtain a practical solution for tall buildings. Samali and Al-Dawod (2003) tested two methods called fuzzy logic controller (FLC) and LQR on a five-story structure model with ATMD under earthquake excitations. Although the performances of the two algorithms are similar, FLC is much better in terms of the number of sensors, computational resources, and the required control power. In another study (Samali et al., 2004), the FLC algorithm was adopted for the ATMD system for vibration control of a 76-story reinforced-concrete office tower in Melbourne, Australia, under crosswind excitation and then compared with a linear quadratic Gaussian (LQG) controller. Like the previous study done by Samali and Al-Dawod (2003), it was concluded that FLC is much better due to the required control power and the number of sensors. H. Kim and Adeli (2004) used a hybrid feedback-least mean square algorithm for ATMDs. H. Kim and Adeli (2005) used a hybrid viscous fluid damper-tuned liquid column damper system that is effective as ATMDs for 76-story benchmark building. To limit the oscillations due to seismic excitations, Han and Li (2006) suggested the use of multiple ATMDs (AMTMD) that have the same damping and stiffness coefficients and different mass and control forces. Also, AMTMDs were applied by C. Li and Xiong (2008) to control translational and torsional responses of an asymmetric structure simplified as two degrees of freedom system. A control method combining FLC and genetic algorithm that is one of the metaheuristic algorithms was proposed by Pourzeynali et al. (2007) for the optimum design of ATMDs. In a design of ATMD system, Guclu and Yazici (2008) suggested the usage of proportional-derivative and FLC control algorithms. In the following year, Guclu and Yazici (2009a) introduced a fuzzy PID controller against the earthquake effect on the structures considering nonlinear base–structure interaction effects. Self-tuning FLCs were also investigated for the earthquake excited structures (Guclu & Yazici, 2009b). In 2010, C. Li et al. (2010) presented an optimum design methodology for ATMD systems applied to asymmetric structures to suppress translational and torsional responses. Then, optimum AMTMD parameters were searched for asymmetric structures by considering the SSI (C. Li, 2012). In the study, the minimization of translational and torsional displacement mean square responses was determined as the optimum parameter criteria. Amini et al. (2013) proposed a method using discrete wavelet transform, PSO, and LQR algorithms to obtain optimum control forces for ATMD. LQG controllers were investigated by You et al. (2014) for the control of structural responses due to along-wind loads in a tall building by using the method derived from the theory of Ayorinde and Warburton (1980) in finding optimum parameters of ATMD. Shariatmadar et al. (2014) appli-

cated the interval type-2 FLC to ATMD to reduce structural responses in a building modeled as a single degree of freedom system. Shariatmadar and Muscat Razavi (2014) proposed combining a FLC and PSO for earthquake excited building. A multi-objective adaptive genetic-fuzzy controller was investigated by Soleymani and Khodadad (2014) for adaptive control design of ATMDs against wind load and earthquake excitations. This investigation revealed that the optimum design of ATMD under earthquake loads is not enough under wind loads and vice versa. C. Li and Cao (2015) proposed the hybrid ATMD system against undesirable oscillations due to ground accelerations. In addition to this, HATMD system was enhanced by linking a dashpot between the structure and ATMD masses (Cao & Li, 2018). Heidari et al. (2018) introduced a hybrid control approach combining PID with LQR to improve the traditional LQR control algorithm. Zelleke and Matsagar (2019) proposed an energy-based predictive algorithm that can be applied to structural control applications and demonstrated it with semi-ATMDs.

Metaheuristic algorithms that are inspired by a phenomenon were employed to optimize controller parameters of active tendon control systems that include the consideration of SSI (Ulusoy et al., 2020) and robustness (Ulusoy et al., 2021). Kayabekir et. al. (2020a) proposed a harmony search (HS)-based methodology for optimum design of ATMDs that do not consider physical conditions like delaying of control signal and limitation of maximum active control force. Even though the optimum values of the method proposed by Kayabekir et al. (2020a) were verified for the time delay in another study (Kayabekir et al., 2020b), the consideration of the time delay is not controlled during the tuning process of the damper and controller parameters. In the realistic design of control systems, the consideration of the factors such as time delay, stroke capacity, and limitation of the control forces are needed to generate a feasible control system. In that case, the final performance of the system can be correctly observed via the solutions, while the performance can be seen as incorrectly superior if these factors are not considered. The main advantage of this study is to consider the three factors in the optimization process of ATMD by checking multiple algorithms for validation of the results.

The presented study is aimed to develop a feasible optimization methodology for ATMDs by the consideration of the delay of the control signal, the limitation of the maximum value of control force, and the maximum allowed stroke capacity of ATMD. The optimization of ATMD system was provided via a novel hybrid algorithm that combines the specific features of HS, flower pollination algorithm (FPA), teaching-learning-based optimization (TLBO) and Jaya algorithm (JA).

In this paper, the methodology is given in Section 2. Section 3 includes the multi-case investigation of a 10-story structure for different time-delay and stroke limitation cases. Also, a 76-story structure was optimized via ATMD to show the capacity of the method. Finally, the conclusions are given in Section 4.

2 | METHODOLOGY

The equations of motion of structure with ATMD are solved by using MATLAB with Simulink (2018). This analysis code is integrated with the iterative metaheuristic-based optimization code. A hybrid algorithm is proposed to combine the effective features of four algorithms. Multiple earthquake records have been considered during optimization. The difficulties of optimization of ATMD as an active control system are also discussed. To avoid these difficulties, the integrated optimization methodology considering the time-delay effect and limitation of the control force is presented.

2.1 | Equations of motion for active-controlled structure

The coupled equations of the structure are shown in matrix form with the interaction of stiffness and damping force resulting via ATMD and the control force that is generated by the employed control algorithm. An n-story building can be defined by n degrees if a degree is considered for lateral movement of each story. With the implementation of ATMD on the top, the system will be an $n + 1$ degrees of freedom system as seen in Figure 1. The governing matrices in the equation of motion and the model of the building are given for a building frame with no rotation of a horizontal section at the level of the rigid floors and columns with fixed at both ends by assuming that the total masses are concentrated at the story levels, but the method can be applied to any system with different structure of system matrices.

For structures under earthquake excitation, TMDs are generally positioned on the top story of the structure because of the existence of the maximum amplitude of the first mode shape at this point. The equations of motion can be written as a single matrix equation as shown in Equation (1). Mass (m_i), stiffness (k_i) and damping coefficient (c_i) of ith story are, respectively, used in the matrices of mass (M), stiffness (K) and damping (C). All these matrices are multiplied with the corresponding derivative of the displacement vector ($x(t)$) including the displacements with respect to the ground for each story (x_i for $i = 1$ to N)
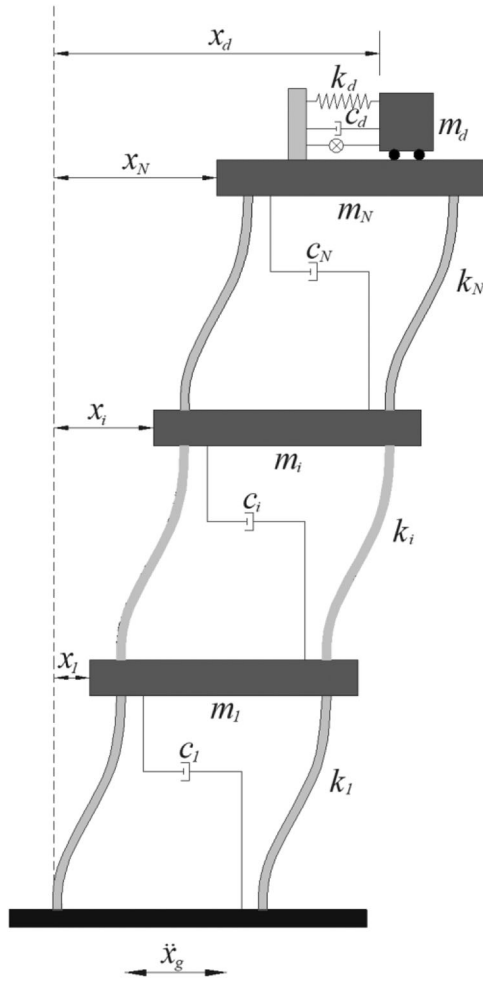
FIGURE 1 A building with active tuned mass damper (ATMD)

$$C = \begin{bmatrix} (c_1 + c_2) & -c_2 \\ -c_2 & (c_2 + c_3) & -c_3 \\ & & \cdot & \cdot \\ & & & \cdot & \cdot & \cdot \\ & & & & \cdot & \cdot & \cdot \\ & & & & & -c_N & (c_N + c_d) & -c_d \\ & & & & & & -c_d & c_d \end{bmatrix} \quad (3)$$

$$K = \begin{bmatrix} (k_1 + k_2) & -k_2 \\ -k_2 & (k_2 + k_3) & -k_3 \\ & & \cdot & \cdot \\ & & & \cdot & \cdot & \cdot \\ & & & & \cdot & \cdot & \cdot \\ & & & & & -k_N & (k_N + k_d) & -k_d \\ & & & & & & -k_d & k_d \end{bmatrix} \quad (4)$$

$$x(t) = \begin{Bmatrix} x_1 \\ x_2 \\ \vdots \\ x_N \\ x_d \end{Bmatrix} \quad (5)$$

$$F(t) = \begin{Bmatrix} 0 \\ 0 \\ \vdots \\ F_u \\ -F_u \end{Bmatrix} \quad (6)$$

and ATMD (x_d). A unit vector ({1}) is used to define story earthquake forces by multiplying it with M and the external excitation defined as ground acceleration time history ($\ddot{x}_g$) resulting from earthquakes. The parameters of ATMD are shown as m_d, k_d, and c_d, which are the mass, stiffness, and damping of ATMD, respectively. $F(t)$ is the control force vector including the generated force by the control system (F_u). All matrices and vectors of Equation (1) are shown as Equations (2)–(6):

$$M\ddot{x}(t) + C\dot{x}(t) + Kx(t) = -M\{1\}\ddot{x}_g(t) + F(t) \quad (1)$$

$$M = \text{diag}\,[m_1 m_2 \dots m_N m_d] \quad (2)$$

The control force is produced by multiplying of trust constant (K_f) and current of armature coil (i_{ATMD}) as seen in Equation (7). In this equation, i_{ATMD} is found according to Equation (8), which includes R as the resistance value, K_e as the induced voltage constant of armature coil, $u(t - td)$ as the delayed control signal with time delay (td). The velocity of top story ($\dot{x}_N$) and ATMD ($\dot{x}_d$) are also used in Equation (8). The control signal is generated via a controller algorithm, which is provided with a PID controller by optimizing the tuning parameters of it:

$$F_u = K_f i_{ATMD} \quad (7)$$

$$Ri_{ATMD} + K_e(\dot{x}_d - \dot{x}_N) = u(t - td) \quad (8)$$

The control signal ($u(t)$) is generated by using PID controllers in the proposed optimum active control system.

PID controllers use three specific actions to transform an error signal into a control signal. The error signal is obtained with the feedback of the response of the system, which is collected via sensors in the time domain. In the present study, the top story velocity was taken as the error signal because the velocity of the structure is directly related to the kinetic energy of the structure under seismic excitations. The actions are processed as proportional, derivative, and integral actions as shown in Equation (9). In Equation (9), these actions have three parameters such as proportional gain (K_p), derivative time (T_d), and integral time (T_i). The active control is provided by tuning these parameters and the performance is dependent on the tuning method. The actions of the PID controller are effective for different purposes. The speed of control response is increased with the help of proportional action. Derivative action provides effective damping, while steady-state errors are eliminated by Integral action (De Cock et al., 1997):

$$u(t) = K_p \left[e(t) + T_d \frac{de(t)}{dt} + \frac{1}{T_i} \int e(t)dt \right] \quad (9)$$

PID controllers are typically used in industry to control processes. For tuning of parameters, several classical methods were developed, which generally depend on trial and error operations. In the documented methods for active control of structures, the other control algorithms generally outperformed PID controllers. As an example (Guclu, 2006), sliding mode control outperforms PID controllers tuned according to the well-known method of Ziegler and Nichols (1942). Contrary to this, a numerical algorithm that scans a defined solution range by constant steps was proposed by Nigdeli and Boduroglu (2013) for tuning PID controllers for active tendon control of structures under near-fault earthquake excitations. Although the proposed numerical algorithm by Nigdeli and Bodruoğlu (2013) is effective, it is needed to find a suitable solution range for the PID parameters to scan. In that situation, a range is needed for time efficiency and preventing stability errors in the loops of the numerical algorithm. Therefore, metaheuristic-based tuning methods have been developed (Ulusoy et al., 2020, 2021) for tuning of PID controllers employed in active structural control using tendons. According to the results of these studies, PID controllers and metaheuristics as the tuning tool of the parameters are proven as an effective method. In this study, the metaheuristic-based tuning of PID controllers is improved to provide a more challenging goal that considers both optimizations of controller and mass damper parameters.

2.2 | The optimization problem

Optimization is a process that proposes the values of design variables, which are the best set of options to minimize or maximize an objective function. Metaheuristic algorithms are applied by several steps, and the essential steps of optimization are iteratively applied.

The optimization problem has five design variables. The mass of ATMD was taken as a constant value because it is generally optimum for the maximum of the range. The other ATMD parameters such as k_d and c_d are considered in Equations (10) and (11) as the period (T_{atmd}) and damping ratio (ξ_d) of ATMD, and these two parameters are defined as design variables. In addition to the physical parameters of ATMD, the other variables used in the optimization of the PID controller are K_p, T_d, and T_i. A set of design variables (X) are shown in Equation (12):

$$T_{atmd} = 2\pi \sqrt{\frac{m_d}{k_d}} \quad (10)$$

$$\xi_d = \frac{c_d}{2\mathrm{m}_d \sqrt{\frac{k_d}{m_d}}} \quad (11)$$

$$X = \left\{ T_{\mathrm{ATMD}} \; \xi_d \; K_p \; T_d \; T_i \right\}^T \quad (12)$$

Two optimization objectives are used in the proposed methodology. The first one is related to a response of the structure, and it is aimed to be minimized. The response is taken as the displacement of the top story (x_N), where the ATMD is placed. For an n-story structure, the first objective function ($f_1(X)$) is written as Equation (13). As shown in Equation (13), a penalty function ($pen(X)$) is also added to the objective function. The penalty is related to the maximum control signal to consider a cost-efficiency and feasible optimum design. During any step of the time-history analysis, if the maximum allowed value of the control force ($F_{\max}$) is exceeded, the analysis for this iteration is terminated for time-saving, and the maximum amount of the control force is added in Newton to the value of the top-story displacement in meter. Since the limit of the control force is extremely big comparing to the displacement values, these solutions are easily eliminated in the iterative optimization process. If the value of the calculated maximum control force is lower than the desired value, pen is taken as zero. When a weighting factor between displacement and force is considered, the optimum solutions

slightly violate the control force constraint. It is the reason for using a penalty function as described in this paper. Since the maximum control forces are big values, compared to the values of the displacement, these results are eliminated in the iterative process of the optimization. pen is formulated as Equation (14).

The secondary objective function ($f_2(X)$) is related to the stroke capacity of ATMD. This function can be also considered as a design constraint, but it is used as a secondary function, and the comparison of existing results is done according to this function if the value of it is more than stmax that is a user-defined value. This objective is formulated as Equation (15). In this formulation, the stroke of controlled structure is checked for all intervals and maximum of it is taken for the ATMD-controlled structure ($\max(|x_d - x_N|)_{\text{withcontrol}}$), and it is normalized according to maximum displacement value of the top story of the structure without any active or passive control system ($\max(|x_N|)_{\text{withoutcontrol}}$). By taking the stroke capacity as an objective, it is possible to scan design variables that have $f_2(X)$ values exceeding stmax. Since $f_2(X)$ is first considered, the search area will be around the nearly exceeded results. This is effective on the convergence of the method on finding the best value of $f_1(X)$ that is usually obtained for the most possible maximum value of stroke if it is limited with a low value. All objectives are calculated by using the values of the design variables that are randomly generated in each iteration and population, and these functions are written as a function of these values. The consideration process of the optimization objectives is presented in Section 2.5.

$$f_1(X) = \max |x_N| + pen(X) \tag{13}$$

$$pen(X) = \begin{cases} 0 & \text{if } \max |F_u| < F_{\max} \\ \max |F_u| & \text{if } \max |F_u| > F_{\max} \end{cases} \tag{14}$$

$$f_2(X) = \frac{\max(|x_d - x_N|)_{\text{with control}}}{\max(|x_N|)_{\text{without control}}} < \text{stmax} \tag{15}$$

2.3 | The earthquake excitations

During the optimization process, both objective functions are calculated for various earthquake records. The maximum ones are considered as the value of the objective functions and eliminations in the iterations that are performed considering the critical one. The usage of multiple excitations is needed to verify the robustness of optimum results since an optimum solution may be a non-effective result for the other one. Additionally, the performance must be

verified by using different excitations since the exact earthquake records are not predicted. Another factor is the possibility of the change of the critical excitation for randomly assigned candidate design variables. To be systematic, a presented set of far fault ground motion records shown in Table 1 were used in optimization (FEMA, 2009).

2.4 | Difficulties in metaheuristic-based optimum design of control systems

As known from TMD optimization studies, the optimum period of TMD is assigned with a close value to the critical period of the main structure. A range between 0.8 and 1.2 times of the period of the main structures is generally chosen (Bekdas et al., 2019). Also, the range of damping ratio is selected as a reasonable value with a maximum of 30%.

For the PID controller parameters, it is hard to define a range. Also, several combinations of PID controller parameters may provide an unstable system in the dynamic analysis. In that case, the iterative optimization process is interrupted. To avoid it, a small range may be defined by trial and error methods, but only a local part of a combination of PID parameters is scanned in this situation. Although the best part of the range is found, a set of PID parameters may result in a big control force value. For that reason, the control force must be limited, and it must be considered as a design constraint. As the best choice, several applications are integrated during the dynamic analysis of structures with active control to shorten the computation time and prevent the interruption of the process.

In the proposed methodology, the displacement response used in the first objective function and the control forces are checked for each time interval. For each time step, the results are checked with the limit values to understand that the randomly defined combination of design variables is suitable or not to reduce the desired response without violation of the control force. The limit of the displacement for the active-controlled structure is equal to the final maximum value of the uncontrolled structure.

2.5 | The optimization method

In this section, the optimization methodology is explained step by step.

As the first step, the design constants, the ranges of design variables, the earthquake excitations and the required user-defined limits and algorithm parameters are defined. The design constants include the structural

TABLE 1 The earthquake records (FEMA, 2009)

Direction 1	Direction 2	Date	Location
SFERN/PEL090	SFERN/PEL180	1971	San Fernando
FRIULI/A-TMZ000	FRIULI/A-TMZ270	1976	Friuli, Italy
IMPVALL/H-DLT262	IMPVALL/H-DLT352	1979	Imperial Valley
IMPVALL/H-E11140	IMPVALL/H-E11230		
SUPERST/B-ICC000	SUPERST/B-ICC090	1987	Superstition Hills
SUPERST/B-POE270	SUPERST/B-POE360		
LOMAP/CAP000	LOMAP/CAP090	1989	Loma Prieta
LOMAP/G03000	LOMAP/G03090		
MANJIL/ABBAR–L	MANJIL/ABBAR–T	1990	Manjil, Iran
LANDERS/YER270	LANDERS/YER360	1992	Landers
LANDERS/CLW-LN	LANDERS/CLW-TR		
CAPEMEND/RIO270	CAPEMEND/RIO360		Cape Mendocino
NORTHR/MUL009	NORTHR/MUL279	1994	Northridge
NORTHR/LOS000	NORTHR/LOS270		
KOBE/NIS000	KOBE/NIS090	1995	Kobe, Japan
KOBE/SHI000	KOBE/SHI090		
DUZCE/BOL000	DUZCE/BOL090	1999	Duzce, Turkey
HECTOR/HEC000	HECTOR/HEC090		Hector Mine
KOCAELI/DZC180	KOCAELI/DZC270		Kocaeli, Turkey
KOCAELI/ARC000	KOCAELI/ARC090		
CHICHI/CHY101-E	CHICHI/CHY101-N		Chi-Chi, Taiwan
CHICHI/TCU045-E	CHICHI/TCU045-N		

properties as mass, stiffness and damping parameters, the control system parameters such as R, K_f, and K_e, simulation time according to time of earthquake excitations, time delay (t_d), and mass of ATMD (m_d). The required user-defined limits are the control force limit and stmax for stroke capacity. Also, a range is defined for the design variables.

- After the definition of the constant values, an initial solution matrix that is merged via sets of design variables (X) is generated. The number of these sets is equal to the population (imitated as harmony in HS, flower in FPA, student in TLBO). The design variables are randomized within the desired range. The minimum and maximum limits of ith design variable are defined by $X_{i,min}$ and $X_{i,max}$, respectively. The initial values are generated as given in Equation (16) for all algorithms.

$$X_i^{j,0} = X_{i,min} + \text{rand}(1)(X_{i,max} - X_{i,min}) \quad (16)$$

$X_i^{j,0}$ represents the initial candidate solution of ith design variable for the jth vector of the initial solution matrix. rand(1) defines a random number between 0 and 1.

For all set of solutions, the objective functions such as $f_1(X)$ and $f_2(X)$ are calculated according to dynamic analy-

sis using the module summarized in the flowchart given in Figure 2.

In the time-domain analysis, the values of $f_1(X)$ and $f_2(X)$ are calculated for all steps. As seen in Figure 2, two comparisons are done. The first one is the check of the top story displacement of the system with ATMD with the same value of the system without control, but the uncontrolled value is taken for the final maximum value of the analysis and earthquake excitation that have the maximum effect. If the controlled value exceeds the uncontrolled value, it is only a waste of time to continue the dynamic analysis for a corresponding set of variables. The dynamic analysis is terminated, and the $f_1(X)$ value is taken as the value of the stopped time. This value is bigger than the uncontrolled response, and it is easily eliminated as a non-effective solution. For that reason, it will not be recognized as an effective value in comparison to the candidate results. Additionally, similar validation is done for the control force (F_u) by changing the results for all time-interval with the maximum allowed value (F_{max}). For validation of the maximum limit, the dynamic analysis is terminated and the pen value is updated with the last control force value. As the initial value, pen is zero at the start of the analysis. The violated results become significant by adding the pen value to the first objective.

FIGURE 2 Flowchart of the dynamic analyses
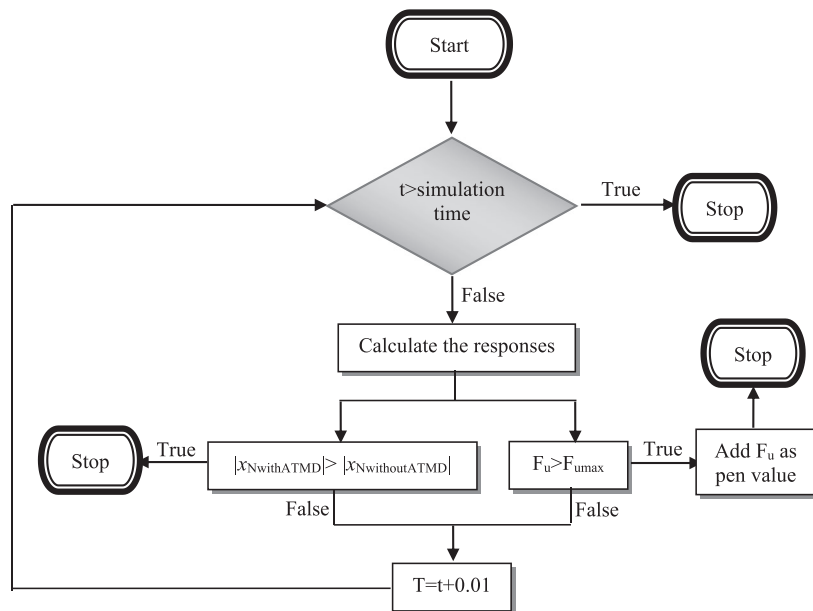
After the generation of the initial solution matrix, the essential optimization process via metaheuristics starts. New sets of design variables are generated via the features of the hybrid algorithm explained in the following sections.

For the design variables such as stiffness, mass, damping coefficient, it is possible to define a suitable solution range to scan the optimum results. In that case, the axial force capacity of the structure and the cost of the control system have limitations for the values of the variables. For the PID controller parameters, a range cannot be defined and PID controller parameters are the weight of different actions. The same control performance can be also found by using different combinations of the variables (Ulusoy et al., 2020, 2021).

Four different metaheuristic algorithms are combined to generate a hybrid algorithm. These metaheuristic algorithms are HS, FPA, TLBO, and JA. These algorithms as the classical forms are proved by the success of optimizing passive (Bekdaş et al., 2019) and active (Kayabekir et al., 2020a; Ulusoy et al., 2020, 2021,) control systems. The unique and different features of the employed algorithms are the main reason for the selection of the algorithms.

HS is a music-inspired metaheuristic algorithm developed by Geem et al. (2001). The unique feature of HS is the usage of harmony memory in the generation of new candidate values. Memory consideration is an effective feature in metaheuristic algorithms, and it can play an important role in local optima problems. An adaptive version of HS was successfully applied on optimization of ATMDs (Kayabekir et al., 2020a), and the adaptive version has active parameter adjusting according to iterations.

FPA developed by X. S. Yang (2012) uses the pollination process of flowering plants. FPA is differentiated by the usage of a Levy distribution in the global pollination process since pollinators obey the rules of Lévy flight.

TLBO is a user-defined parameter-free metaheuristic algorithm developed by Rao et al. (2011). The phases of education as teaching and learning are formulized. In the formulation, a parameter called the teaching factor (TF) is used, but it is not a user-defined parameter. TF is randomly chosen as 1 or 2 in the algorithm. Generally, metaheuristic algorithms need a probability (for example, switch probability in FPA and harmony memory considering rate in HS) to choose one of the optimization types or phases in an iteration. The phases of TLBO are consequently applied in an iteration, and a parameter is not needed.

JA is an algorithm that takes the name "Jaya" from the word meaning victory in Sanskrit. It is also a user-defined parameter-free algorithm developed by Rao et al. (2016). Since it is a single-phase algorithm, it may trap local optima for the problem that considers the optimization of both physical mass damper variables and controller parameters.

To collect all advantages of these four algorithms, a hybrid algorithm is proposed. The algorithm has two phases, and these phases are consequently applied in a single iteration like TLBO.

The first phase of the algorithm is the global search phase. In this phase, both worst and best solutions are used like JA. As the randomization, a Levy distribution is used, but a linear distribution is also provided in several situations. In that case, the randomization is done in two ways to eliminate to trap local optimum or use an improper distribution. In the choice of the type of distribution, TF in TLBO is used, and it is not needed to add a

user-defined parameter. It is formulated as Equation (17), and as described in TLBO, TF is a random value that can be 1 or 2. A new design variable ($X_i^{j,t+1}$) is generated by using both the worst ($w_i^{j,*}$) and best ($g_i^{j,*}$) solution. The values of $i, j,$ and t define design variable ($i = 1$ to n: number of design variables), population ($j = 1$ to p: number of members in population) and iteration ($t = 1$ to mt: maximum number of iteration), respectively. The general formulation in Equation (17) is similar to JA with modification to absolute value operations to increase the convergence ability for the problem that can have positive or negative controller parameters. A Lévy distribution (L) used in the study is given as Equation (18), and r_1 and r_2 are random numbers between 0 and 1:

$$X_i^{j,t+1} = \begin{cases} X_i^{j,t} + L(g_i^{j,*} - X_i^{j,t}) - L(w_i^{j,*} - X_i^{j,t}) & \text{if TF} = 2 \\ X_i^{j,t} + r_1(g_i^{j,*} - X_i^{j,t}) - r_2(w_i^{j,*} - X_i^{j,t}) & \text{if TF} = 1 \end{cases}$$
(17)

$$L = \frac{1}{\sqrt{2p}} (\text{RAND}(1))^{-1.5} e^{\frac{-1}{2rand(1)}}$$
(18)

As the second phase, the memory consideration is used with an adaptive parameter. This parameter is taken from the HS as fret width (fw). Generally in FPA and TLBO, a new solution is reproduced by randomly choosing two existing solutions. In this hybrid algorithm, a single memory is chosen as done in HS, and it is modified according to Equation (19). The initial fw (fw_{in}) value is proposed to be a small value (taken as 0.05 in the study), and it is modified according to iterations as seen in Equation (20). $X_k^{j,t}$ is the kth existing solution in the memory.

$$X_i^{j,t+1} = X_i^{j,t} + (r_1 - 0.5)fwX_i^{j,t}$$

$$fw = fw_{in} + \left(1 - \frac{t}{mt}\right)$$
(19)

After the generation of a new set of design variables, newly generated results are compared with the existing ones. When both new and existing results do not provide $f_2(X) <$ stmax, a set of design variables with the minimum $f_2(X)$ is saved. If one of them provides $f_2 <$ stmax, the providing result is saved. For the other cases, the design variables with minimum $f_1(X)$ are saved. By this operation, all sets of solutions in the solution matrix are updated.

The iterative optimization step continues for a maximum number of iterations, and the process ends after all iterations are done. The flowchart of the optimization process is shown in Figure 3.

3 | NUMERICAL EXAMPLES

The optimum design of the ATMD system attached to the top of a 10-story building was investigated for different stroke limits (stmax) and time delay (td) conditions. Each story of the building is assumed to have the same structural properties. In addition to design variable limits, design constants of the structure and the control system, and other information about the analyzed situations can be also found in Table 2.

The problem was optimized under eight different cases including combinations of two different stroke limits and four different time delays. In the analyses, restrictions on the control force of ATMD are also defined. It is aimed to represent practical applications of the control system. The results are presented and discussed in the following sections. Also, the control methodology was verified on a real-size reinforced concrete space structure.

In the dynamic analysis of the optimization process, the Runge–Kutta method was chosen as the solver. The time step of time-history analyses is taken as 1×10^{-2} s and the analyses were done for 60 s duration.

3.1 | The optimum results

The optimization results are presented in Table 3 that shows the results for different stroke limit (stmax) and time delay (td) conditions for the algorithms. In the tables; f_1 and f_2 represent the objective functions. F_u denotes the maximum control force applied to the building under the critical earthquake record. F_{max} is taken as 10% of the total weight of the structure.

Optimum ATMD parameter values can be summarized as follows:

- For the specific time delay cases, the optimum ATMD damping ratios decrease as stmax increases.
- On the other hand, for stmax = 2 cases, as td increases, the optimum damping ratios increase. For stmax = 3, there is no increment or decrement trend in the optimum damping ratios due to td values.
- Except for 50 ms time delay analyses, optimum ATMD periods increase as stmax values increase. On the other hand, for 50 ms, there is an opposite trend.
- The distribution of optimum ATMD period values is different in cases of time delay for a specific stmax value. According to this; for stmax = 2, no trend was observed in the period values due to the increase in time delay. For stmax = 3, it was observed that the optimum periods decrease as the time delay increased.

FIGURE 3 Flowchart of the optimization methodology
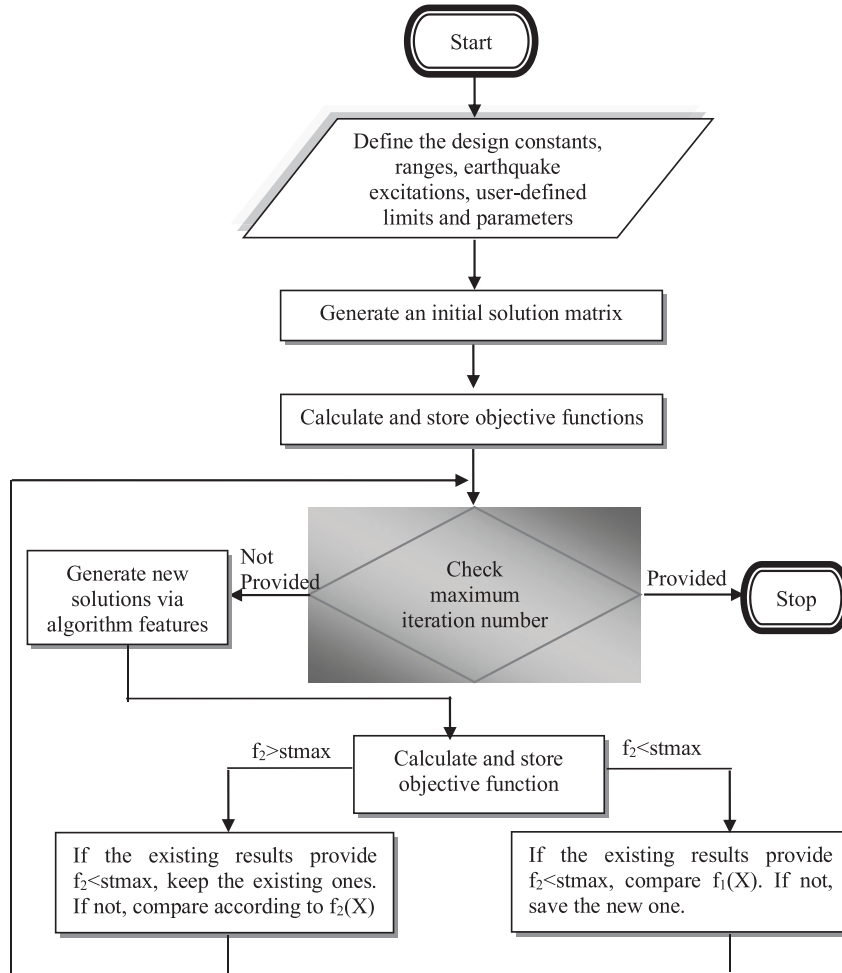
TABLE 2 The constant parameters

Symbol	Definition	Value	Unit
m_i	Mass of the story	360	ton
k_i	Rigidity coefficient of the story	650	MN/m
c_i	Damping coefficient of the story	6.2	MNs/m
m_d	Mass of active tuned mass damper (ATMD)	180	ton
T_{atmd}	Period of ATMD	0.5–1.5 times of structure period	s
ξ_d	Damping ratio of ATMD	1–50	%
K_p	Proportional gain	−10,000–10,000	Vs/m
T_d	Derivative time	−10,000–10,000	s
T_i	Integral time	−10,000–10,000	s
stmax	Stroke limit of ATMD	2, 3	–
td	Time delay	10, 20, 30, 50	ms
R	Resistance value	4.2	Ω
K_f	Trust constant	2	N/A
K_e	Induced voltage constant of armature coil	2	V
pn	Population number	10	–
mt	Maximum iteration number	500	–

TABLE 3 The optimum results for ATMD

	stmax = 2				stmax = 3			
td	10	20	30	50	10	20	30	50
T_{atmd} (s)	0.944	0.9730	0.950	0.962	1.018	1.0216	0.975	0.951
ξ_d (%)	26.281	27.596	28.640	28.488	11.068	11.707	11.920	11.203
K_p (Ns/m)	−206.67	−2907.5	1329.61	50.1541	384.967	−123.050	514.182	−2165
T_d (s)	2588.9	176.715	−417.23	−9904.8	−1353.6	4127	−1055.8	226.90
T_i (s)	−28.749	860.535	−8026.3	−9639.7	−892.39	−8314.2	9328.27	−2413.9
f_2	1.999	1.999	1.999	1.999	2.999	2.999	2.999	2.999
F_u (kN)	3529.3	3525.2	3525.4	3529.76	3529.3	3530.10	3530.11	3526.2
f_1 (m)	0.2498	0.2528	0.2544	0.2612	0.2123	0.2173	0.2200	0.2285

TABLE 4 The optimization results of TMD by modified harmony search (HS)

	TMD	
stmax	2	3
T_{tmd} (s)	0.9418	0.9434
ξ_{tmd} (%)	5.64	4.69
f_2	1.9999	2.0755
f_1 (m)	0.2820	0.2803

• The maximum control forces applied to the structure do not differ greatly according to stmax or td conditions. The biggest difference between the maximum and minimum control forces is 0.14%.

3.2 | The comparison of the active and passive TMDs

In this section, the performance of active and passive mass damper systems is compared. The optimum period (T_{tmd}) and damping ratio (ξ_{tmd}) of TMD considering different stmax values for TMD systems are given in Table 4. Considering the optimum period values, the increasing trend for increasing stmax values except for $td = 50$ in ATMD-controlled cases is also observed in the TMD-controlled cases. Also, decreasing the behavior of damping ratios in the ATMD system due to stmax values is valid for the TMD system. However, it is worth noting that the change of the TMD system is very limited, compared to the ATMD system. Besides, the damping ratio and period values are lower than ATMD-controlled structures. Two important results have been observed regarding the stroke limits of TMD and ATMD systems. First, design constraints values for optimum results are different for TMD and ATMD systems. Second, although the values are equal to the upper limit in ATMD systems, it is only at the upper limit for stmax = 2 in the TMD system. According to this result,

it can be said that more stroke capacity is needed for the ATMD system.

Examining the displacement values of ATMD, the values tend to decrease significantly, compared to stmax cases. On the other hand, the objectives of the TMD system are approximately the same. Another result is that the performance of the ATMD system is better than TMD. The difference between systems varies within 7.95%–12.89% for stmax = 2, and 22.69%–32.01% for stmax = 3.

The critical earthquake in the optimization process is the BOL090 component of the Duzce earthquake record. Under the critical earthquake record, the minimum top story displacements of uncontrolled, TMD-controlled, and ATMD-controlled structures are 0.4101, 0.2802, and 0.2123 m in the stmax = 3, td = 10 cases, respectively, as shown in Figure 4, with time history graphs presented for the critical earthquake excitation. TMD and ATMD systems are very effective in providing a quick steady-state response of the structure by damping vibration effects.

Finally, performance checks of the ATMD system were carried out for the optimum values obtained. The performances of the active control system for other earthquake records were investigated by using the optimum ATMD system parameters, and the results of the top story displacement are given in Table 5.

From Table 5, it is understood that the ATMD system is also quite successful under other earthquake records, compared to the uncontrolled structure and TMD-controlled structure. Especially, the efficiency of ATMD is significant under the excitations causing big displacements.

Additionally, the optimum results were also tested for different earthquake records. Table 6 shows the results of the top-story displacement for the records that are presented as near-field records with a pulse in FEMA P-695 (FEMA, 2009). As seen from Table 6, the optimized ATMD for all time delays is generally effective on the response under different earthquake records that are not taken into consideration during the optimization process. Especially, the best profit of the control system is provided
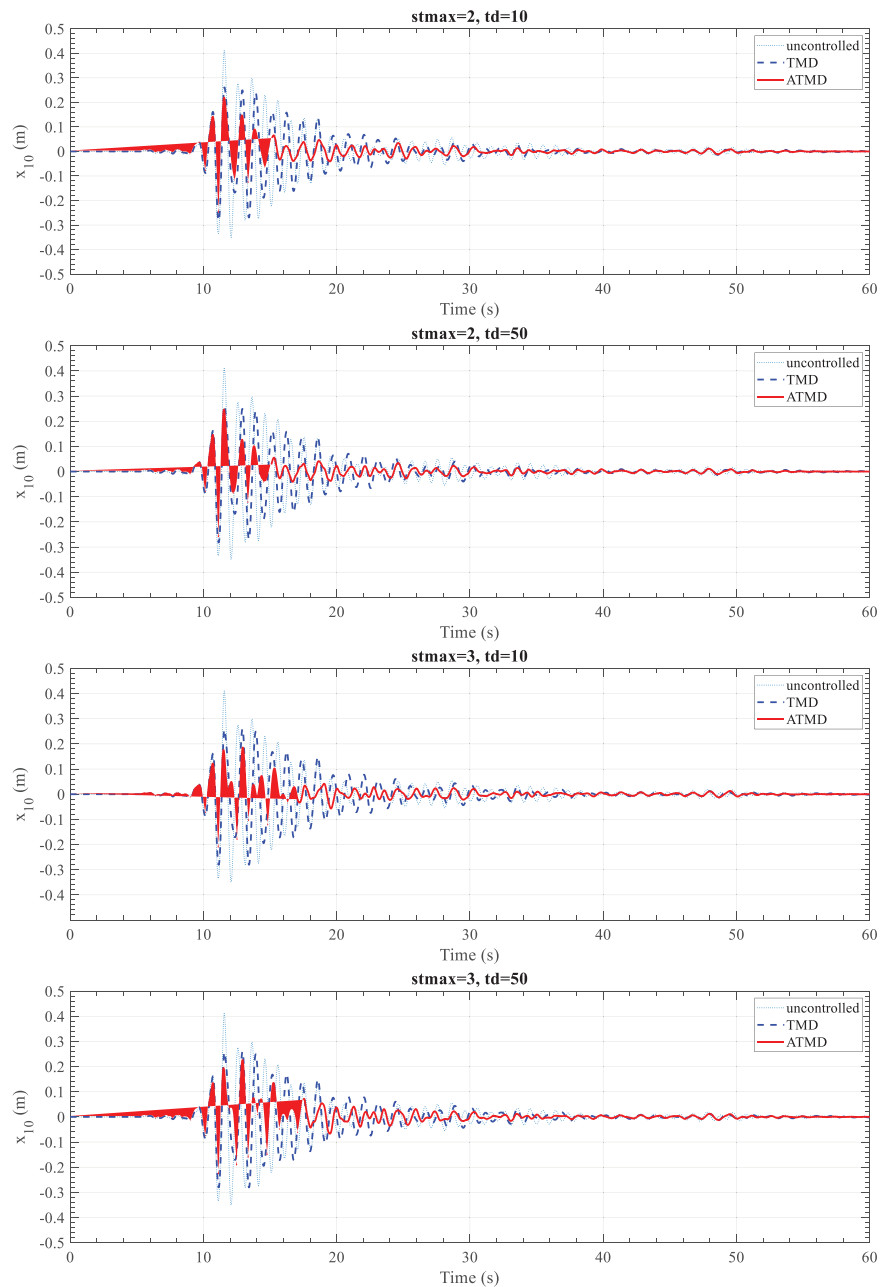
TABLE 5 Maximum top-story displacements (m) for FEMA P-695 far-field ground motions

	Without control	TMD	ATMD stmax = 2				TMD	ATMD stmax = 3			
td (ms)			10	20	30	50	10	20	30	50
NORTHR/MUL009	0.3693	0.2128	0.2141	0.2091	0.2115	0.2124	0.2221	0.1690	0.1758	0.1772	0.1916
NORTHR/MUL279	0.311	0.282	0.2442	0.2473	0.2483	0.2550	0.2802	0.1894	0.1945	0.1953	0.2011
NORTHR/LOS000	0.1326	0.0942	0.0989	0.1009	0.1013	0.1032	0.0931	0.1042	0.1048	0.1037	0.1022
NORTHR/LOS270	0.2236	0.1487	0.1420	0.1462	0.1475	0.1538	0.1467	0.1432	0.1461	0.1539	0.1641
DUZCE/BOL000	0.259	0.1721	0.1482	0.1524	0.1532	0.1598	0.1713	0.1299	0.1350	0.1321	0.1383
DUZCE/BOL090	0.4101	0.282	0.2498	0.2528	0.2544	0.2612	0.2803	0.2123	0.2173	0.2200	0.2285
HECTOR/HEC000	0.1118	0.1585	0.1066	0.1034	0.1042	0.1061	0.1641	0.0967	0.0965	0.1025	0.1082
HECTOR/HEC090	0.1317	0.1617	0.1322	0.1286	0.1292	0.1273	0.1667	0.1315	0.1303	0.1358	0.1384
IMPVALL/H-DLT262	0.111	0.0665	0.0541	0.0576	0.0581	0.0631	0.0685	0.0670	0.0691	0.0671	0.0690
IMPVALL/H-DLT352	0.1894	0.109	0.0959	0.0968	0.0966	0.0982	0.1124	0.0988	0.0977	0.1055	0.1096
IMPVALL/H-E11140	0.0765	0.0624	0.0560	0.0547	0.0550	0.0553	0.0616	0.0579	0.0586	0.0585	0.0559
IMPVALL/H-E11230	0.0705	0.1001	0.0860	0.0861	0.0864	0.0863	0.1015	0.1092	0.1100	0.1122	0.1149
KOBE/NIS000	0.1112	0.1152	0.0914	0.0955	0.0954	0.1001	0.1164	0.0920	0.0966	0.0901	0.0942
KOBE/NIS090	0.1013	0.0951	0.0870	0.0894	0.0900	0.0959	0.0953	0.1049	0.1053	0.1157	0.1258
KOBE/SHI000	0.1045	0.1434	0.1261	0.1262	0.1266	0.1293	0.1445	0.1177	0.1175	0.1225	0.1238
KOBE/SHI090	0.0764	0.1009	0.0783	0.0792	0.0796	0.0810	0.1039	0.0985	0.0997	0.1005	0.1025
KOCAELI/DZC180	0.1547	0.1223	0.1088	0.1104	0.1107	0.1161	0.1213	0.0936	0.0957	0.0962	0.1018
KOCAELI/DZC270	0.2234	0.1972	0.1732	0.1693	0.1697	0.1677	0.1972	0.1605	0.1586	0.1653	0.1669
KOCAELI/ARC000	0.0407	0.0401	0.0272	0.0266	0.0272	0.0292	0.0408	0.0297	0.0299	0.0306	0.0324
KOCAELI/ARC090	0.0396	0.0341	0.0316	0.0321	0.0317	0.0324	0.035	0.0413	0.0416	0.0410	0.0410
LANDERS/YER270	0.1797	0.1289	0.1199	0.1180	0.1177	0.1178	0.1284	0.1250	0.1255	0.1245	0.1283
LANDERS/YER360	0.1139	0.0828	0.0750	0.0740	0.0746	0.0744	0.0832	0.0791	0.0780	0.0770	0.0770
LANDERS/CLW-LN	0.0834	0.0833	0.0662	0.0668	0.0675	0.0705	0.0848	0.0688	0.0704	0.0740	0.0804
LANDERS/CLW-TR	0.1369	0.1498	0.1371	0.1385	0.1390	0.1409	0.1516	0.1642	0.1635	0.1728	0.1790
LOMAP/CAP000	0.1467	0.1673	0.1456	0.1409	0.1416	0.1440	0.1705	0.1732	0.1679	0.1862	0.1940
LOMAP/CAP090	0.0949	0.1065	0.0996	0.1014	0.1020	0.1032	0.1137	0.1223	0.1227	0.1260	0.1258
LOMAP/G03000	0.1139	0.0749	0.0712	0.0733	0.0732	0.0721	0.0749	0.0716	0.0732	0.0723	0.0715
LOMAP/G03090	0.1223	0.1394	0.1189	0.1202	0.1207	0.1246	0.1436	0.1165	0.1185	0.1195	0.1252
MANJIL/ABBAR–L	0.1236	0.0814	0.0821	0.0881	0.0878	0.0967	0.081	0.1016	0.1045	0.0988	0.1009
MANJIL/ABBAR–T	0.1847	0.1471	0.1274	0.1281	0.1273	0.1277	0.1474	0.1068	0.1086	0.1044	0.1073
SUPERST/B-ICC000	0.0848	0.1541	0.1401	0.1394	0.1390	0.1404	0.1561	0.1522	0.1527	0.1523	0.1552
SUPERST/B-ICC090	0.0837	0.0959	0.0770	0.0742	0.0744	0.0736	0.0974	0.0835	0.0811	0.0804	0.0808
SUPERST/B-POE270	0.1151	0.1291	0.0747	0.0747	0.0737	0.0746	0.1325	0.0814	0.0807	0.0789	0.0785
SUPERST/B-POE360	0.1374	0.1269	0.0821	0.0798	0.0794	0.0811	0.1321	0.0833	0.0835	0.0845	0.0896
CAPEMEND/RIO270	0.1829	0.154	0.1395	0.1413	0.1421	0.1473	0.1533	0.1323	0.1345	0.1382	0.1468
CAPEMEND/RIO360	0.1398	0.1173	0.0959	0.0938	0.0949	0.1010	0.1166	0.0840	0.0845	0.0859	0.0934
CHICHI/CHY101-E	0.1608	0.1079	0.0901	0.0928	0.0924	0.1007	0.1121	0.1013	0.1023	0.1082	0.1155
CHICHI/CHY101-N	0.3546	0.208	0.1848	0.1859	0.1871	0.1943	0.2055	0.1459	0.1483	0.1553	0.1650
CHICHI/TCU045-E	0.1085	0.0836	0.0715	0.0753	0.0763	0.0791	0.0845	0.0815	0.0824	0.0831	0.0819
CHICHI/TCU045-N	0.1514	0.1238	0.1151	0.1173	0.1173	0.1214	0.1228	0.1127	0.1142	0.1130	0.1171
SFERN/PEL090	0.0851	0.0823	0.0599	0.0587	0.0585	0.0583	0.0844	0.0684	0.0684	0.0600	0.0626
SFERN/PEL180	0.0614	0.0349	0.0296	0.0304	0.0303	0.0325	0.036	0.0282	0.0286	0.0288	0.0307
FRIULI/A-TMZ000	0.0847	0.0614	0.0527	0.0530	0.0539	0.0550	0.0608	0.0602	0.0618	0.0574	0.0600
FRIULI/A-TMZ270	0.1013	0.0851	0.0748	0.0764	0.0770	0.0802	0.0847	0.0837	0.0830	0.0929	0.0968

FIGURE 4 Time histories of the top-story displacements under critical earthquake record

for the RRS228 component of the Rinaldi record of the 1994 Northridge earthquake. For this excitation, the maximum top-story displacement for the uncontrolled structure is 0.6457 m, while it can be reduced to 0.5077 and 0.5068 m by using TMDs that are optimized for stmax = 2 and stmax = 3, respectively. The ATMD-controlled systems for stmax = 2 are effective to reduce the maximum displacement to 0.4694, 0.4750, 0.4758, and 0.4868 m for td values of 10, 20, 30, and 50 ms, respectively. For stmax = 3, these values change between 0.4502 and 0.4689 m with the increase of td. The significant importance of ATMD against TMD is clearly seen since ATMD is also effective on several records such as B-PTS225 and TCU065-E that have also high effects on TMD-controlled structures.

3.3 | 76-story high-rise structure

The application of the method was employed to find an optimum ATMD that is positioned on a high-rise structure that cannot be easily controlled by several options like base isolators and friction dampers. The investigated structure is a slender building with a width ratio of 7.3. The structural model was first introduced by Yang et al. (1998). The details of the plan of the 76-story reinforced concrete office building are given in Yang et al. (2004). The 76-story building is 306 m tall and the total mass of the building is 153,000 tons.

In this application, td was taken as 20 ms as an average value. Two cases of stmax were done for cases as stmax = 2

TABLE 6 Maximum top-story displacements (m) for FEMA P-695 near-field ground motions with pulse

	Without control	TMD	ATMD stmax = 2				TMD stmax = 3		ATMD			
td (ms)			10	20	30	50			10	20	30	50
H-E06140	0.2159	0.1486	0.1159	0.1175	0.1159	0.1194	0.1550	0.1637	0.1663	0.1606	0.1680
H-E06230	0.1509	0.1424	0.1383	0.1405	0.1404	0.1420	0.1429	0.1441	0.1458	0.1432	0.1435
H-E07140	0.2254	0.1820	0.1622	0.1638	0.1646	0.1699	0.1828	0.1668	0.1695	0.1717	0.1800
H-E07230	0.2302	0.2124	0.1984	0.2008	0.2011	0.2060	0.2121	0.1942	0.1968	0.1969	0.2026
A-STU000	0.1045	0.1008	0.0898	0.0900	0.0892	0.0896	0.1021	0.1008	0.1011	0.0996	0.1017
A-STU270	0.1546	0.1187	0.1064	0.1077	0.1068	0.1110	0.1188	0.1051	0.1068	0.1054	0.1117
B-PTS225	0.3562	0.3736	0.2649	0.2549	0.2543	0.2510	0.3852	0.2830	0.2855	0.2895	0.3084
B-PTS315	0.1702	0.2058	0.1514	0.1482	0.1494	0.1523	0.2109	0.1710	0.1730	0.1808	0.1967
STG000	0.1538	0.1635	0.1409	0.1360	0.1362	0.1325	0.1656	0.1434	0.1429	0.1522	0.1557
STG090	0.1281	0.0744	0.0693	0.0708	0.0711	0.0753	0.0725	0.0545	0.0556	0.0569	0.0605
ERZ-EW	0.1957	0.1841	0.1700	0.1713	0.1711	0.1740	0.1839	0.1629	0.1647	0.1644	0.1687
ERZ-NS	0.2837	0.2370	0.2112	0.2131	0.2130	0.2173	0.2350	0.1989	0.2011	0.2008	0.2061
PET000	0.2135	0.1842	0.1678	0.1748	0.1768	0.1865	0.1842	0.1770	0.1834	0.1812	0.1891
PET090	0.3367	0.2945	0.2624	0.2682	0.2700	0.2823	0.2936	0.2483	0.2553	0.2559	0.2681
LCN260	0.1372	0.2027	0.1788	0.1796	0.1799	0.1818	0.2049	0.1904	0.1937	0.1978	0.2057
LCN345	0.1086	0.0844	0.0662	0.0667	0.0689	0.0727	0.0874	0.0607	0.0612	0.0636	0.0681
RRS228	0.6457	0.5077	0.4694	0.4750	0.4758	0.4865	0.5068	0.4502	0.4565	0.4567	0.4689
RRS318	0.2700	0.2193	0.1982	0.2046	0.2072	0.2173	0.2184	0.2011	0.1985	0.2080	0.2166
SYL090	0.2137	0.1910	0.1799	0.1881	0.1864	0.1929	0.1945	0.2048	0.2098	0.1890	0.1890
SYL360	0.2716	0.2767	0.2440	0.2421	0.2430	0.2480	0.2754	0.2110	0.2139	0.2129	0.2209
IZT090	0.1105	0.0669	0.0677	0.0678	0.0682	0.0683	0.0673	0.0753	0.0753	0.0761	0.0766
IZT180	0.1141	0.0569	0.0474	0.0465	0.0470	0.0475	0.0567	0.0405	0.0404	0.0421	0.0445
TCU065-E	0.4373	0.4228	0.2805	0.2742	0.2807	0.2841	0.4258	0.2084	0.2006	0.2085	0.2306
TCU065-N	0.4048	0.3150	0.2224	0.2259	0.2268	0.2343	0.3293	0.2394	0.2441	0.2446	0.2629
TCU102-E	0.1912	0.2237	0.1812	0.1747	0.1757	0.1745	0.2248	0.1895	0.1897	0.1964	0.2038
TCU102-N	0.2293	0.1792	0.1273	0.1194	0.1208	0.1192	0.1824	0.1150	0.1130	0.1270	0.1383
DZC180	0.1925	0.1476	0.1071	0.1113	0.1128	0.1194	0.1543	0.1152	0.1219	0.1115	0.1181
DZC270	0.2878	0.1686	0.1471	0.1551	0.1541	0.1671	0.1762	0.1875	0.1938	0.1783	0.1789

TABLE 7 The optimization results of ATMD by modified HS

stmax	2	3
T_{atmd} (s)	4.5752	4.9723
ξ_d (%)	15.06	9.14
K_p	-3.784×10^3	5.589×10^3
T_d (s)	568.274	-384.884
T_i (s)	-5.904×10^3	-718.473

and stmax = 3. The mass of ATMD was taken as 1530 t. The optimum design variables found via the modified HS are listed in Table 7.

The most critical excitation occurs under CHICHI/ CHY101-N record of the 1999 Chi-Chi, Taiwan, earthquake. The uncontrolled response with 4.58-m displacement reduces to 4.005 and 3.928 m for the cases of stmax = 2 and stmax = 3, respectively.

4 | CONCLUSION

In the study, the optimum design of the ATMD system was searched for the minimization of maximum displacements using a hybrid algorithm. The optimum design conducted for different stroke limits (stmax) and time delay (td) conditions under the critical earthquake were determined for the FEMA P-695 far-field ground motions. Comparative analysis performed under several cases of 10-story structure via the developed method for the ATMD system revealed two important results. One of them is the better performance of ATMD (up to 32.01%) than TMD under all earthquakes considering the optimization process. It must be noted that this performance was provided for an optimum design of ATMD that has optimum T_{atmd} and ξ_d values that are different from the values of optimum TMD. Another result is related to the importance of

the stroke capacity consideration of ATMD optimization. Since stroke values are at the upper bounds of the optimization for optimum ATMD, it is found as ATMDs need more stroke than TMDs.

Additionally, a 76-story high-rise reinforced concrete structure was considered as the employed method to add an ATMD on the top of the building. According to the results, it is seen that the optimum damping ratio of ATMD is nearly double for limited stroke capacity as stmax = 2. The examined stmax cases have slightly different optimum periods. For the proportional action of the PID controller, K_d values are different in the sign of the values for different stmax values and also have T_d values with the different signs, but the derivative action is similar since it includes multiplication of K_d and T_d. The integral actions and T_i values are very different. Because of the big T_i value, integral action has a small impact in control for stmax = 2. The proposal is feasible and effective on major structures that cannot be easily controlled via well-known and economical control applications.

Compared to other control algorithms, the proposed methodology is a direct-tuning of ATMDs by employing time-domain responses under various numbers of excitations by controlling reference values for the capacity of the control system including the limitation of the control force, stroke, minor delays of the control system. With the development of such control applications, it will be possible to promote more effective and economical control applications in the world.

REFERENCES

Adeli, H., & Park, H. S. (1995). A neural dynamics model for structural optimization—Theory. *Computers & structures*, *57*(3), 383–390.

Aldemir, U., & Bakioglu, M. (2001). Active structural control based on the prediction and degree of stability. *Journal of Sound and Vibration*, *247*(4), 561–576.

Aldemir, U., Bakioglu, M., & Akhiev, S. S. (2001). Optimal control of linear buildings under seismic excitations. *Earthquake Engineering and Structural Dynamics*, *30*(6), 835–851.

Amini, F., Hazaveh, N. K., & Rad, A. A. (2013). Wavelet PSO-based LQR algorithm for optimal structural control using active tuned mass dampers. *Computer-Aided Civil and Infrastructure Engineering*, *28*(7), 542–557.

Ankireddi, S., Yang, H. T. Y. (1996). Simple ATMD control methodology for tall buildings subject to wind loads. *Journal of Structural Engineering*, *122*(1), 83–91.

Arfiadi, Y., & Hadi, M. N. S. (2000). Passive and active control of three-dimensional buildings. *Earthquake Engineering and Structural Dynamics*, *29*(3), 377–396.

Ayorinde, E. O., & Warburton, G. B. (1980). Minimizing structural vibrations with absorbers. *Earthquake Engineering and Structural Dynamics*, *8*(3), 219–236.

Bakioglu, M., & Aldemir, U. (2001). A new numerical algorithm for sub-optimal control of earthquake excited linear structures. *International Journal for Numerical Methods in Engineering*, *50*(12), 2601–2616.

Bekdaş, G., Kayabekir, A. E., Nigdeli, S. M., & Toklu, Y. C. (2019). Tranfer function amplitude minimization for structures with tuned mass dampers considering soil-structure interaction. *Soil Dynamics and Earthquake Engineering*, *116*, 552–562.

Cao, L., & Li, C. (2018). Enhanced hybrid active tuned mass dampers for structures. *Structural Control and Health Monitoring*, *25*(2), e2067.

Chang, C. -C., & Lin, C. (2009). H_∞ drift control of time-delayed seismic structures. *Earthquake Engineering and Engineering Vibration*, *8*(4), 617–626.

De Cock, K., De Moor, B., Minten, W., Van Brempt, W., & Verrelst, H. (1997). *A tutorial on PID-control, ESAT-SISTA/TR 1997-08*. Department of Electrical Engineering, Katholieke Universiteit Leuven.

FEMA (2009). *P-695: Quantification of building seismic performance factors*. US Department of Homeland Security, FEMA.

Geem, Z. W., Kim, J. H., & Loganathan, G. V. (2001). A new heuristic optimization algorithm: harmony search. *Simulation*, *76*(2), 60–68.

Guclu, R. (2006). Sliding mode and PID control of a structural system against earthquake. *Mathematical and Computer Modelling*, *44*(1-2), 210–217.

Guclu, R., & Yazici, H. (2008). Vibration control of a structure with ATMD against earthquake using fuzzy logic controllers. *Journal of Sound and Vibration*, *318*(1-2), 36–49.

Guclu, R., & Yazici, H. (2009a). Seismic-vibration mitigation of a nonlinear structural system with an ATMD through a fuzzy PID controller. *Nonlinear Dynamics*, *58*(3), 553.

Guclu, R., & Yazici, H. (2009b). Self-tuning fuzzy logic control of a non-linear structural system with ATMD against earthquake. *Nonlinear Dynamics*, *56*(3), 199.

Han, B., & Li, C. (2006). Seismic response of controlled structures with active multiple tuned mass dampers. *Earthquake Engineering and Engineering Vibration*, *5*(2), 205–213.

Heidari, A. H., Etedali, S., & Javaheri-Tafti, M. R. (2018). A hybrid LQR-PID control design for seismic control of buildings equipped with ATMD. *Frontiers of Structural and Civil Engineering*, *12*(1), 44–57.

Jiang, X., & Adeli, H. (2008). Dynamic fuzzy wavelet neuroemulator for nonlinear control of irregular highrise building structures. *International Journal for Numerical Methods in Engineering*, *74*(7), 1045–1066.

Kayabekir, A. E., Bekdaş, G., Nigdeli, S. M., & Geem, Z. W. (2020a). Optimum design of PID controlled active tuned mass damper via modified harmony search. *Applied Sciences*, *10*(8), 2976.

Kayabekir, A. E., Nigdeli, S. M., & Bekdaş, G. (2020b). Robustness of structures with active tuned mass dampers optimized via modified harmony search for time delay. *International conference on harmony search algorithm*, Istanbul, Turkey (pp. 53–60).

Kim, H., & Adeli, H. (2004). Hybrid feedback-least mean square algorithm for structural control. *Journal of Structural Engineering*, *130*(1), 120–127.

Kim, H., & Adeli, H. (2005). Wind-induced motion control of 76-story benchmark building using the hybrid damper-tuned liquid column damper system. *Journal of Structural Engineering*, *131*(12), 1794–1802.

Kim, Y., Langari, R., & Hurlebus, S. (2010). Model-based multi-input, multi-output supervisory semiactive nonlinear fuzzy controller. *Computer-Aided Civil and Infrastructure Engineering*, *25*(5), 387–393.

Li, C. (2012). Effectiveness of active multiple-tuned mass dampers for asymmetric structures considering soil–structure interaction effects. *The Structural Design of Tall and Special Buildings*, *21*(8), 543–565.

Li, C., & Cao, B. (2015). Hybrid active tuned mass dampers for structures under the ground acceleration. *Structural Control and Health Monitoring*, *22*(4), 757–77.

Li, C., Li, J., & Qu, Y. (2010). An optimum design methodology of active tuned mass damper for asymmetric structures. *Mechanical Systems and Signal Processing*, *24*(3), 746–765.

Li, C., & Xiong, X. (2008). Estimation of active multiple tuned mass dampers for asymmetric structures. *Structural Engineering and Mechanics*, *29*(5), 505–530.

Li, Z., & Adeli, H. (2016). New discrete-time robust H_2/H_∞ algorithm for vibration control of smart structures using linear matrix inequalities. *Engineering Applications of Artificial Intelligence*, *55*, 47–57.

Li, Z., & Adeli, H. (2018). Control methodologies for Vibration Control of Smart Civil and Mechanical Structures. *Expert Systems*, *35*(6), e12354.

Lin, C., Chang, C., & Wang, J. (2010). Active control of irregular buildings considering soil-structure interaction effects. *Soil Dynamics and Earthquake Engineering*, *30*(3), 98–109.

Lu, J., & Skelton, R. E. (1998). Optimal hybrid control for structures. *Computer-Aided Civil and Infrastructure Engineering*, *13*(6), 405–414.

Mackriell, L. E., Kwok, K. C. S., & Samali, B. (1997). Critical mode control of a wind-loaded tall building using an active tuned mass damper. *Engineering Structures*, *19*(10), 834–842.

MATLAB (2018). 9.7. 0.1190202 (R2019b), Natick, Massachusetts: The MathWorks Inc. https://www.mathworks.com/products/new_products/release2019b.html

Nigdeli, S. M., & Boduroğlu, M. H. (2013). Active tendon control of torsionally irregular structures under near-fault ground motion excitation. *Computer-Aided Civil and Infrastructure Engineering*, *28*(9), 718–736.

Nomura, Y., Furuta, H., & Hirokane, M. (2007). An integrated fuzzy control system for structural vibration. *Computer-Aided Civil and Infrastructure Engineering*, *22*(4), 306–316.

Pourzeynali, S., Lavasani, H. H., & Modarayi, A. H. (2007). Active control of high rise building structures using fuzzy logic and genetic algorithms. *Engineering Structures*, *29*(3), 346–357.

Qu, Z. Q., Shi, Y., & Hua, H. (2001). A reduced-order modeling technique for tall buildings with active tuned mass damper. *Earthquake Engineering & Structural Dynamics*, *30*(3), 349–362.

Rao, R. V., Savsani, V. J., & Vakharia, D. P. (2011). Teaching–learning-based optimization: a novel method for constrained mechanical design optimization problems. *Computer-Aided Design*, *43*(3), 303–315.

Rao, R. (2016). Jaya: A simple and new optimization algorithm for solving constrained and unconstrained optimization problems. *International Journal of Industrial Engineering Computations*, *7*(1), 19–34.

Saleh, A., & Adeli, H. (1994). Parallel algorithms for integrated structural and control optimization. *Journal of Aerospace Engineering*, *7*(3), 297–314.

Saleh, A., & Adeli, H. (1998). Optimal control of adaptive/smart building structures. *Computer-Aided Civil and Infrastructure Engineering*, *13*(6), 389–403.

Samali, B., & Al-Dawod, M. (2003). Performance of a five-storey benchmark model using an active tuned mass damper and a fuzzy controller. *Engineering Structures*, *25*(13), 1597–1610.

Samali, B., Al-Dawod, M., Kwok, K. C., & Naghdy, F. (2004). Active control of cross wind response of 76-story tall building using a fuzzy controller. *Journal of Engineering Mechanics*, *130*(4), 492–498.

Shariatmadar, H., Golnargesi, S., & Akbarzadeh Totonchi, M. R. (2014). Vibration control of buildings using ATMD against earthquake excitations through interval type-2 fuzzy logic controller. *Asian Journal of Civil Engineering-Building and Housing*, *15*(3), 321–338.

Shariatmadar, H., & Razavi, H. M. (2014). Seismic control response of structures using an ATMD with fuzzy logic controller and PSO method. *Structural Engineering and Mechanics*, *51*(4), 547–564.

Soleymani, M., & Khodadadi, M. (2014). Adaptive fuzzy controller for active tuned mass damper of a benchmark tall building subjected to seismic and wind loads. *The Structural Design of Tall and Special Buildings*, *23*(10), 781–800.

Soto, M. G., & Adeli, H. (2017a). Many-objective control optimization of high-rise building structures using replicator dynamics and neural dynamics model. *Structural and Multidisciplinary Optimization*, *56*(6), 1521–1537.

Soto, M. G., & Adeli, H. (2017b). Recent advances in control algorithms for smart structures and machines. *Expert Systems*, *34*(2), e12205.

Soto, M. G., & Adeli, H. (2018). Vibration control of smart base-isolated irregular buildings using neural dynamic optimization model and replicator dynamics. *Engineering Structures*, *156*, 322–336.

Soto, M. G., & Adeli, H. (2019). Semi-active vibration control of smart isolated highway bridge structures using replicator dynamics. *Engineering Structures*, *186*, 536–552.

Ulusoy, S., Bekdas, G., & Nigdeli, S. M. (2020). Active structural control via metaheuristic algorithms considering soil-structure interaction. *Structural Engineering and Mechanics*, *75*(2), 175–191.

Ulusoy, S., Nigdeli, S. M., & Bekdaş, G. (2021). Novel metaheuristic-based tuning of PID controllers for seismic structures and verification of robustness. *Journal of Building Engineering*, *33*, 101647.

Wang, N., & Adeli, H. (2015a). Robust vibration control of wind-excited highrise building structures. *Journal of Civil Engineering and Management*, *21*(8), 967–976.

Yan, N., Wang, C. M., & Balendra, T. (1999). Optimal damper characteristics of ATMD for buildings under wind loads. *Journal of Structural Engineering*, *125*(12), 1376–1383.

Yang, J. N., Agrawal, A. K., Samali, B., & Wu, J. C. (2004). Benchmark problem for response control of wind-excited tall buildings. *Journal of Engineering Mechanics*, *130*(4), 437–446.

Yang, J. N., Wu, J. C., Samali, B., & Agrawal, A. K. (1998). A benchmark problem for response control of wind-excited tall buildings. *Proceedings of the 2nd World Conference on Structural Control*, Kyoto, Japan (pp. 1407–1416).

WILEY |

Yang, X. S. (2012). Flower pollination algorithm for global optimization. In J. Durand-Lose, & N. Jonoska (Eds.). *International conference on unconventional computing and natural computation* (pp. 240–249). Springer.

You, K. P., You, J. Y., & Kim, Y. M. (2014). LQG control of along-wind response of a tall building with an ATMD. *Mathematical Problems in Engineering*, *2014*, 206786.

Zelleke, D. H., & Matsagar, V. A. (2019). Semi-active algorithm for energy-based predictive structural control using tuned mass dampers. *Computer-Aided Civil and Infrastructure Engineering*, *34*(11), 1010–1025.

Ziegler, J. G., & Nichols, N. B. (1942). Optimum settings for automatic controllers. *Transactions of the ASME*, *64*(11), 759–765.